Inorganica Chimica Acta, 211 (1993) 221–226

$HgCl_2$ coordination to guanine derivatives: structural and spectroscopic studies on the interactions with 9-ethylguanine, 1,9-dimethylguanine and 2-amino-6-methoxy-9-methylpurine (6,9-dimethylguanine)

Stephan Menzer, Edda C. Hillgeris and Bernhard Lippert*
Fachbereich Chemie, Universität Dortmund, D-44221 Dortmund (Germany)

(Received May 8, 1993)

Abstract

The coordination of $HgCl_2$ to 9-ethylguanine, 1,9-dimethylguanine and 2-amino-6-methoxy-9-methylpurine (6,9-dimethylguanine) has been studied. The X-ray structures of the complexes $HgCl_2$ (2-amino-6-methoxy-9-methylpurine-*N7*) (**1**) (monoclinic, $P2_1/m$, $a = 10.160(3)$, $b = 6.222(1)$, $c = 11.060(3)$ Å, $\beta = 116.11(2)°$, $Z = 2$) and $\{[HgCl_2\cdot(1,9\text{-dimethyl-guanine-}N7)]_2HgCl_2\}_n$ (**2**) (orthorhombic, *Pbca*, $a = 6.955(2)$, $b = 17.176(6)$, $c = 21.829(9)$ Å, $Z = 4$) are reported. Binding of $HgCl_2$ is through N7 of the purine bases. In **1** discrete molecules are formed, while **2** is a linear polymer with $(Hg–Cl)_n$ chains to which the guanine bases and chloro ligands are coordinated. The solution behavior is characterized by a rapid ligand exchange and low complex formation constants, log $\beta_1 = 0.4$ (**1**), 1.3 (1:1 adduct of **2**) and 1.0 [$HgCl_2\cdot$9-EtGH] (**3**).

Introduction

X-ray structurally characterized examples of mercury complexes with nucleobases or closely related ligands such as cyclic amides can be categorized as follows: (i) compounds of $[CH_3Hg^{II}]^+$ with essentially linear Hg coordination geometries [1], (ii) compounds with Hg^{II} bound to two (identical) nucleobases [2, 3] or related ligands [4] in a colinear fashion, (iii) $HgCl_2$ adducts with rather versatile coordination numbers of mercury, ranging from 3 to 6 and frequently irregular geometries [5–10], and (iv) a compound with a nearly linear $L–Hg^I–Hg^I–L$ arrangement [11].

Herewith, we report the X-ray structures of two $HgCl_2$ adducts with 2-amino-6-methoxy-9-methylpurine (6,9-dimethylguanine, 6,9-DiMeG) and 1,9-dimethylguanine (1,9-DiMeG), respectively.

Experimental

Chemicals

9-Ethylguanine (9-EtGH), 1,9-dimethylguanine (1,9-DiMeG) and 2-amino-6-methoxy-9-methylpurine (6,9-DiMeG) were obtained from Chemogen (Konstanz, Germany). Ethanediol and glycerol (Fluka) were used as received. Me_2SO (Fluka) and $Me_2SO\text{-}d_6$ (Merck) were dried using CaH_2 and 3 Å molecular sieves, respectively.

Preparation

The following complexes were prepared using gel growth crystallization techniques: $HgCl_2\cdot$6,9-DiMeG (**1**); $\{[HgCl_2\cdot1,9\text{-DiMeG}]_2HgCl_2\}_n$ (**2**) and $HgCl_2\cdot$9-EtGH (**3**). An outline of the general procedure applied is given in ref. 12. The guanine ligand was dissolved in ethanediol (6,9-DiMeG; 9-EtGH) or glycerol (1,9-DiMeG). $HgCl_2$ in all cases was in the aqueous phase. Details of the various preparations are given in Table 1. The yields strongly depended on the reaction time. Single crystals were obtained within days in low yields (<5%), while microcrystals were formed in high yield (>80%) if the mixtures were allowed to stand for 14 days or even longer. Single crystals and microcrystalline products were identical on the basis of their IR spectra and elemental analysis.

Anal. Calc. for $C_7H_9N_5Cl_2HgO$ (**1**): C, 18.7; H, 2.0; N, 15.5. Found: C, 18.5; H, 2.0; N, 15.4%. IR data (KBr, cm^{-1}): 3480w, 3420s, 3300s, 3180s, 3090w, 2920w, 1640vs, 1590vs, 1520s, 1470s, 1450w, 1410s, 1370vs, 1350w, 1330w, 1280w, 1240s, 1060s, 940w, 770s, 690w, 680w, 610w, 420w.

Anal. Calc. for $C_{14}H_{18}N_{10}Hg_3Cl_6O_2$ (**2**): C, 14.3; H, 1.6; N, 11.9. Found: C, 14.3; H, 1.5; N, 11.9%. IR data

---

*Author to whom correspondence should be addressed.

0020-1693/93/$6.00

TABLE 1. Preparations of **1**–**3**

Complex	Components	Volume (ml)	Solvent[a]	Mass (mg)	Concentration (mmol)	Method[b]
1	$HgCl_2$	2.5	H_2O	22.3	0.08	A
	6,9-DiMeG	2.5	I	15.2	0.08	
2	$HgCl_2$	5	H_2O	16.3	0.06	B
	1,9-DiMeG	5	II	27.6	0.15	
3	$HgCl_2$	5	H_2O	14.9	0.05	A
	9-EtGH	5	I	9.8	0.05	

[a] I = ethanediol, II = glycerol. [b] A = test tube, no filter paper; B = test tube with filter paper between the phases.

(KBr, cm^{-1}): 3400w, 3300w, 3190w, 3090w, 1690vs, 1610vs, 1560s, 1530s, 1430s, 1380w, 1190w, 1060w, 1010w, 860w, 770w, 700w, 650w, 610w, 480w, 380w, 330w.

Anal. Calc. for $C_7H_9N_5Cl_2HgO$ (**3**): C, 18.7; H, 2.0; N, 15.5. Found: C, 18.6; H, 1.9; N, 15.3%. IR data (KBr, cm^{-1}): 3400w, 3310w, 3210w, 3100w, 1690vs, 1650s, 1600w, 1580s, 1530s, 1410w, 1360s, 1210w, 1180s 1080w, 1010w, 970w, 770w, 710w, 680w, 620w, 430w.

Instrumentation

IR spectra were recorded on a Perkin-Elmer 580-B spectrometer using KBr pellets. ^{199}Hg NMR spectra were recorded using Bruker AM300 (53.481 MHz) and AC 200 (35.654 MHz) instruments (25 °C, 10 and 5 mm tubes, 95% Me_2SO, 5% Me_2SO-d_6). Chemical shifts are given in ppm and are referenced to external 0.1 M $HgCl_2/Me_2SO$ (-1500 ppm relative external Me_2Hg). The method of calculation of complex formation constants using concentration dependent NMR spectra was reviewed in ref. 13. The calculations were performed on an ATARI-ST computer.

X-ray crystallography

The crystal structures of **1** and **2** were determined on a Nicolet R3m/V diffractometer with graphite monochromated Mo Kα radiation ($\lambda = 0.71073$ Å) and solved using the computer programs SHELXTL PLUS [14] and PARST [15]. The data were corrected for absorption effects. Crystallographic data are given in Table 2. Atomic scattering factors for neutral atoms and real and imaginary dispersion terms were taken from the International Tables for X-ray Crystallography [16]. Atomic coordinates of the non H-atoms are given in Tables 3 and 4. H atoms were not located.

TABLE 2. Experimental data for the X-ray study of **1** and **2**

	1	**2**
Formula	$C_7H_9N_5Cl_2HgO$	$C_{14}H_{18}N_{10}Hg_3Cl_6O_2$
Crystal system	monoclinic	orthorhombic
Space group	$P2_1/m$	$Pbca$
a (Å)	10.160(3)	6.955(2)
b (Å)	6.222(1)	17.176(6)
c (Å)	11.060(3)	21.829(9)
β (°)	116.11(2)	
V (Å^3)	627.6(3)	2606.4(17)
Z	2	4
D_{calc} (g cm^{-3})	2.384	2.989
μ (Mo Kα) (mm^{-1})	12.672	18.277
F_w (g mol^{-1})	450.68	1172.75
F(000) (e)	416	2120
T (°C)	20	20
Radiation	Mo Kα	Mo Kα
λ (Å)	0.71073	0.71073
Monochromator	graphite	graphite
Index range	$-12 \leqslant h \leqslant 12$ $0 \leqslant k \leqslant 7$ $-13 \leqslant l \leqslant 13$	$-9 \leqslant h \leqslant 9$ $0 \leqslant k \leqslant 21$ $-26 \leqslant l \leqslant 26$
Reflections measured	2425	7525
Reflections unique	1224	2308
R_{int}	12.9	2.19
Reflections observed ($F_o > 4\sigma(F_o)$)	1144	1586
Parameters refined	97	160
R	3.60	2.85
R_w	4.05	3.28
Goodness-of-fit	2.02	1.24
Δ_{fin}(max.) (e Å^{-3})	1.03	0.89
2θ Range (°)	2–50	2–50

Results

Description of the structure of 1

The structure of the neutral complex $HgCl_2 \cdot$6,9-DiMeG is shown in Fig. 1 and selected intramolecular distances and angles are given in Table 5. Non-H atoms are on a crystallographic mirror plane and therefore the molecule is strictly planar. Binding of Hg is through N(7) of the guanine, while the N(1) position is not affected. This donor site is not protonated under neutral conditions. The methyl substituent at O(6) of the nucleobase adopts the usual *trans* conformation relative to the C5–C6 bond, very much as in the free ligand [17], in 6,9-dimethyladenine [18] or in a Pt complex of the latter [19]. The steric bulk of the CH_3 group certainly does not favor Hg binding at N(1). The N(7)–Hg(1) bond length (2.09(1) Å) is somewhat

TABLE 3. Atomic coordinates ($\times 10^4$) and equivalent isotropic displacement coefficients ($Å^2 \times 10^3$) for **1**

	x	y	z	U_{eq}[a]
Hg(1)	1287(1)	2500	9965(1)	40(1)
Cl(1)	1099(3)	2500	7807(3)	51(1)
Cl(2)	−1481(2)	2500	9706(2)	38(1)
N(7)	2140(8)	2500	12064(8)	28(3)
C(8)	1380(11)	2500	12783(10)	32(4)
N(9)	2260(9)	2500	14114(7)	30(3)
C(9)	1801(14)	2500	15215(11)	49(5)
N(1)	6192(9)	2500	14023(9)	36(3)
C(2)	6113(12)	2500	15240(10)	33(4)
N(2)	7416(10)	2500	16338(9)	44(4)
N(3)	4884(9)	2500	15427(8)	33(3)
C(4)	3695(10)	2500	14292(9)	27(4)
C(5)	3602(10)	2500	12992(9)	29(3)
C(6)	4926(11)	2500	12889(10)	32(4)
O(6)	4873(8)	2500	11702(7)	42(3)
C(61)	6273(15)	2500	11556(14)	78(7)

[a]Equivalent isotropic U defined as one third of the trace of the orthogonalized U_{ij} tensor.

TABLE 4. Atomic coordinates ($\times 10^4$) and equivalent isotropic displacement coefficients ($Å^2 \times 10^3$) for **2**

	x	y	z	U_{eq}[a]
Hg(1)	2169(1)	2007(1)	623(1)	32(1)
Hg(2)	5000	0	0	44(1)
Cl(1)	5854(4)	1857(2)	146(1)	31(1)
Cl(3)	4631(6)	201(2)	−1025(1)	48(1)
Cl(2)	869(5)	857(2)	261(1)	43(1)
N(1)	2596(12)	2135(4)	2873(4)	22(1)
C(1)	2188(18)	1439(6)	3249(5)	31(3)
C(2)	3187(16)	2820(6)	3128(5)	26(4)
N(2)	3259(14)	2861(5)	3758(4)	34(4)
N(3)	3637(13)	3469(4)	2821(4)	25(3)
C(4)	3533(15)	3368(5)	2195(4)	19(3)
C(5)	3027(16)	2708(5)	1898(4)	17(3)
C(6)	2471(14)	2036(6)	2210(4)	23(3)
O(6)	1935(12)	1413(4)	1993(3)	33(3)
N(7)	3067(13)	2835(4)	1277(4)	26(3)
C(8)	3622(17)	3576(5)	1203(5)	28(4)
N(9)	3956(13)	3915(4)	1759(4)	25(3)
C(9)	4620(21)	4711(6)	1867(6)	46(3)

[a]Equivalent isotropic U is defined as one third of the trace of the orthogonalized U_{ij} tensor.

shorter than in similar complexes with 9-methylhypoxanthine [9] (2.299(7) Å) and guanosine [8] (2.16(2) Å). The coordination sphere of Hg is distorted trigonal planar with respect to its two inequivalent chlorine ligands and N(7). The Hg(1)–O(6) separation (3.29 Å) is not to be considered a bond. In the crystal lattice the complexes are stacked along a twofold screw axis, which is parallel to the crystallographic b axis. This leads to the formation of additional weak Hg–Cl contacts of 3.13(3) Å, thereby extending the coordination sphere to a distorted and very much elongated trigonal bipyramid (Cl′–Hg–Cl″, 168°). Two bases on the same side of the screw axis partly overlap with a base from a neighboring chain (Fig. 2). The overall appearance

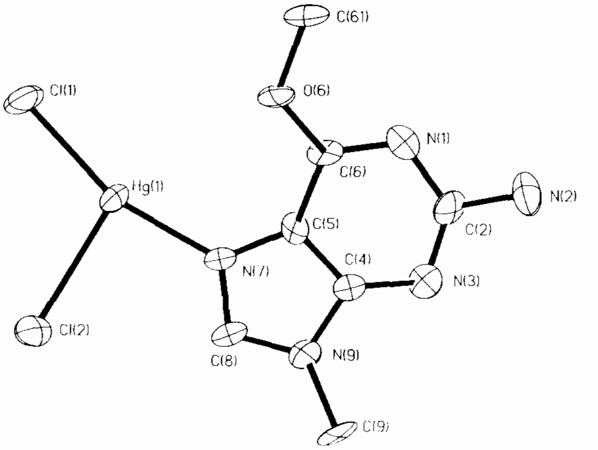

Fig. 1. View of $HgCl_2$(6,9-DiMeG) (**1**) with atom numbering.

TABLE 5. Selected bond lengths (Å) and angles (°) for **1**

Hg(1)–Cl(1)	2.309(3)	Hg(1)–Cl(2)	2.699(3)
Hg(1)–N(7)	2.091(8)	N(7)–C(8)	1.329(16)
N(7)–C(5)	1.385(10)	C(8)–N(9)	1.345(11)
N(9)–C(9)	1.484(18)	N(9)–C(4)	1.382(14)
N(1)–C(2)	1.384(16)	N(1)–C(6)	1.344(11)
C(2)–N(2)	1.346(11)	C(2)–N(3)	1.353(17)
N(3)–C(4)	1.304(10)	C(4)–C(5)	1.398(15)
C(5)–C(6)	1.400(16)	C(6)–O(6)	1.290(14)
O(6)–C(61)	1.500(19)		
Cl(1)–Hg(1)–Cl(2)	106.4(1)	Cl(1)–Hg(1)–N(7)	162.4(3)
Cl(2)–Hg(1)–N(7)	91.2(3)	Hg(1)–N(7)–C(8)	126.8(6)
Hg(1)–N(7)–C(5)	127.4(8)	C(8)–N(7)–C(5)	105.8(8)
N(7)–C(8)–N(9)	111.9(9)	C(8)–N(9)–C(9)	126.9(9)
C(8)–N(9)–C(4)	107.9(10)	C(9)–N(9)–C(4)	125.2(7)
C(2)–N(1)–C(6)	117.8(10)	N(1)–C(2)–N(2)	115.0(11)
N(1)–C(2)–N(3)	127.0(8)	N(2)–C(2)–N(3)	118.0(10)
C(2)–N(3)–C(4)	112.3(10)	N(9)–C(4)–N(3)	127.5(11)
N(9)–C(4)–C(5)	105.3(7)	N(3)–C(4)–C(5)	127.2(11)
N(7)–C(5)–C(4)	109.1(10)	N(7)–C(5)–C(6)	134.1(10)
C(4)–C(5)–C(6)	116.8(8)	N(1)–C(6)–C(5)	118.9(10)
N(1)–C(6)–O(6)	122.9(11)	C(5)–C(6)–O(6)	118.2(8)
C(6)–O(6)–C(61)	119.5(8)		

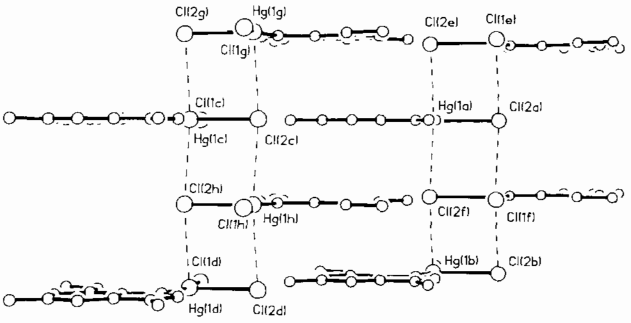

Fig. 2. Packing of molecules of **1** along the a axis. Axial Hg...Cl contacts are indicated by broken lines.

of **1** thus is similar to the structure of $HgCl_2 \cdot$guanosine [8] as far as base stacking is concerned, but the interactions of Hg with the 'axial' chlorides are considerably weaker in our case.

There are no significant differences in the geometry of the free ligand [17] and the purine base in **1**, except for the C(6)–O(6) bond which shortens (1.290(14) Å) upon $HgCl_2$ binding to N(7) (1.340(2) Å in free base).

Description of the structure of 2

Figure 3 depicts the asymmetric unit of the polymeric complex $\{[HgCl_2 \cdot 1,9\text{-DiMeG}]_2HgCl_2\}_n$. Selected bond distances and angles are given in Table 6. Again, Hg binds through N(7) of the purine, with a bond length (2.110(8) Å) which is comparable to that in **1**. The coordination sphere of Hg is completed by three Cl ligands. One of these, Cl(2), has a normal bond distance to Hg of 2.312(3) Å, while bond lengths to the two other chlorides Cl(1) (2.779(3) Å), Cl(1a) (2.730(3) Å), are long as a consequence of their bridging functions. Hg(1) is not coplanar with N(7), Cl(1) and Cl(2), as in the case of **1**. Rather, Cl(1a) is the fourth ligand of a distorted tetrahedron around the metal. As indicated in Fig. 4, there is a relatively short contact of 3.37 Å between Hg and N of the NH_2(2) group of an adjacent guanine ligand. Since the lone pair of the amino group of guanine is delocalized into the aromatic system and therefore not available to function as a donor for the metal, the possibility of an NH...Hg hydrogen bond formation as found in a number of other cases [20] cannot be fully ruled out, although the coplanarity of the NH_2 protons with the guanine ring is not too favorable. However, such an interaction is restricted to the solid state only.

As also evident from Fig. 4, guanine rings of adjacent chains costack efficiently.

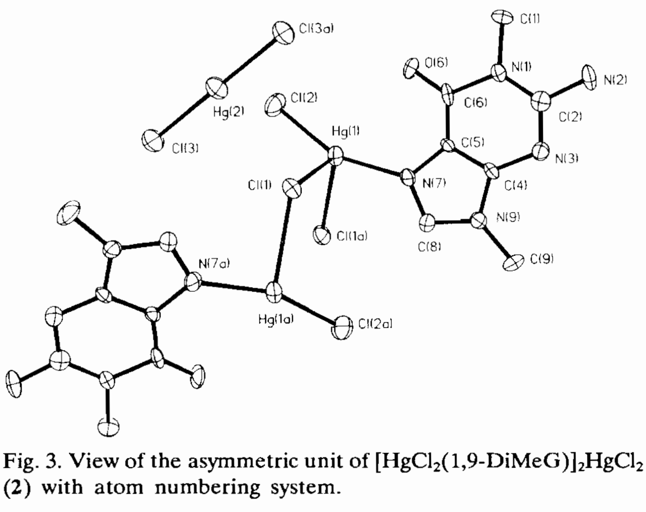

Fig. 3. View of the asymmetric unit of $[HgCl_2(1,9\text{-DiMeG})]_2HgCl_2$ (**2**) with atom numbering system.

TABLE 6. Selected bond lengths (Å) and angles (°) for **2**

Hg(1)–Cl(1)	2.779(3)	Hg(1)–Cl(2)	2.312(3)
Hg(1)–N(7)	2.110(8)	Hg(1)–Cl(1a)	2.730(3)
Hg(2)–Cl(3)	2.279(3)	N(1)–C(1)	1.476(12)
N(1)–C(2)	1.364(12)	N(1)–C(6)	1.460(12)
C(2)–N(2)	1.377(14)	C(2)–N(3)	1.338(13)
N(3)–C(4)	1.379(13)	C(4)–C(5)	1.352(13)
C(4)–N(9)	1.369(12)	C(5)–C(6)	1.394(13)
C(5)–N(7)	1.374(13)	C(6)–O(6)	1.228(12)
N(7)–C(8)	1.339(12)	C(8)–N(9)	1.366(13)
N(9)–C(9)	1.463(13)		
Cl(1)–Hg(1)–Cl(2)	98.8(1)	Cl(1)–Hg(1)–N(7)	92.5(3)
Cl(2)–Hg(1)–N(7)	157.4(2)	Cl(1)–Hg(1)–Cl(1a)	98.3(1)
Cl(2)–Hg(1)–Cl(1a)	105.6(1)	N(7)–Hg(1)–Cl(1a)	91.9(2)
Cl(3)–Hg(2)–Cl(3a)	180.0	Hg(1)–Cl(1)–Hg(1a)	118.2(1)
C(1)–N(1)–C(2)	121.9(8)	C(1)–N(1)–C(6)	116.4(7)
C(2)–N(1)–C(6)	121.5(8)	N(1)–C(2)–N(2)	117.6(9)
N(1)–C(2)–N(3)	125.7(10)	N(2)–C(2)–N(3)	116.7(9)
C(2)–N(3)–C(4)	112.3(8)	N(3)–C(4)–C(5)	126.4(9)
N(3)–C(4)–N(9)	126.2(8)	C(5)–C(4)–N(9)	107.3(8)
C(4)–C(5)–C(6)	122.1(9)	C(4)–C(5)–N(7)	109.5(8)
C(6)–C(5)–N(7)	128.2(8)	N(1)–C(6)–C(5)	111.8(8)
N(1)–C(6)–O(6)	120.2(8)	C(5)–C(6)–O(6)	128.0(9)
Hg(1)–(N7)–C(5)	123.7(6)	Hg(1)–N(7)–C(8)	130.0(7)
C(5)–N(7)–C(8)	106.1(8)	N(7)–C(8)–N(9)	110.2(9)
C(4)–N(9)–C(8)	106.8(8)	C(4)–N(9)–C(9)	126.7(8)
C(8)–N(9)–C(9)	126.4(8)		

Figure 5 gives yet another view of the crystal lattice, indicating the position and function of the cocrystallized $HgCl_2$. The molecule is linear with Hg(2)–Cl(3) bonds of 2.279(3) Å. In addition, Hg(2) forms four long contacts with Cl(2) (3.278(3) Å) and Cl(1) (3.259(3) Å), thereby linking the polymeric *catena*-(μ-chloro)-chloro(1,9-dimethylguanine-*N*7) mercury(II) chains.

As compared to the free purine nucleobase [17], there are no significant changes in ligand geometry upon Hg binding.

$HgCl_2$(9-EtGH)

$HgCl_2$ forms a 1:1 complex with 9-EtGH. Mercury binding should also be through N(7), which is the most basic donor site of the purine. Coordination via O(6) is unlikely as evident from the IR spectra (νCO is not shifted upon coordination). Therefore a structure analogous to that of **1** can be assumed.

^{199}Hg NMR studies

The results of the ^{199}Hg NMR titrations are plotted in Fig. 6. Although large shift differences are observed upon addition of the purine ligands, no individual signals of the solvated $HgCl_2$ and the guanine complexes are observed. This indicates that the ligand exchange is very fast. The complex formation constant log β_1 can be evaluated from the concentration dependencies of the chemical shift data (Table 7). Log β_1 values are

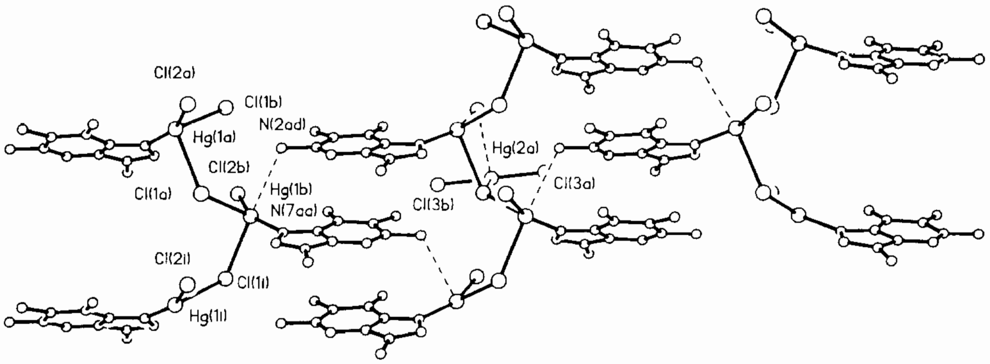

Fig. 4. Packing of compound **2**. Close intermolecular contacts between Hg(1) and the amino group of 1,9-DiMeG are indicated by broken lines.

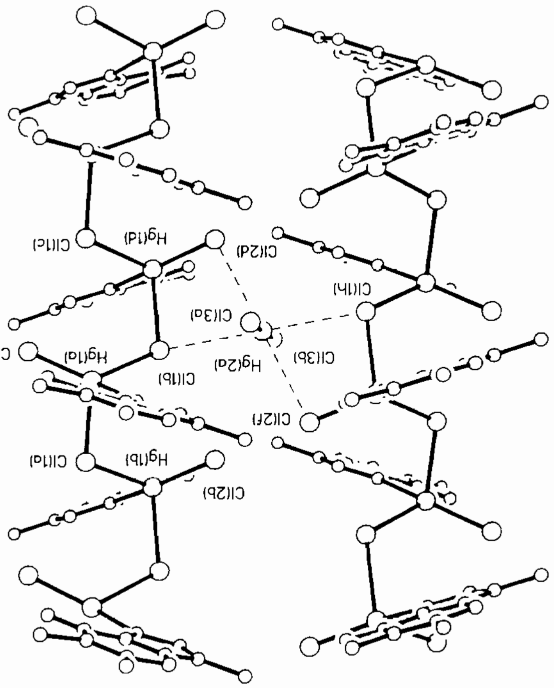

Fig. 5. Different view of packing of **2** (along *b* axis) with $HgCl_2$ linking infinite $HgCl_2$(1,9-DiMeG) chains through weak Cl...Hg contacts.

small, as expected for simple 'adduct' formation of $HgCl_2$. The values obtained compare well with that for the $HgCl_2$/guanosine system [21]. Much higher stability constants can be expected if Hg^{II} (without Cl ligands) binds to nucleobases.

We are aware that the 1:1 model applied may be oversimplified, since only reactions in the first coordination sphere of Hg can be detected while the formation of a chlorine bridged polymer might result in effects which are small compared with the shift differences due to guanine complexation. On the other hand, an analysis based on the assumption that both 1:1 and 1:2 complexes are present in solution did not fit the experimental data.

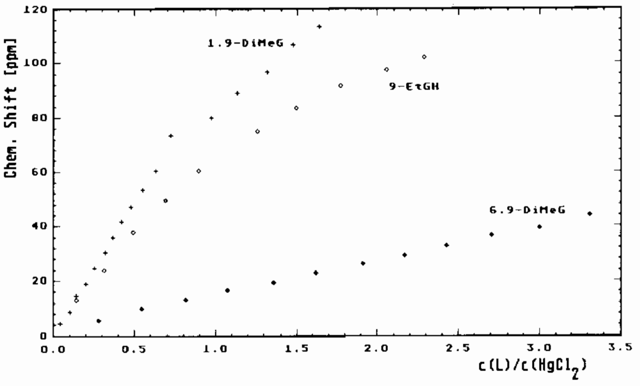

Fig. 6. ^{199}Hg NMR chemical shifts vs. concentration of the guanine nucleobase (Me_2SO; $c(HgCl_2) = 0.1$ M).

TABLE 7. Complex formation constants and maximum ^{199}Hg NMR chemical shift differences (relative to $HgCl_2$)

	log β_1	Δ_{max} (ppm)
$HgCl_2 \cdot$ 6,9-DiMeG	0.4^b	219
$HgCl_2 \cdot$ 1,9-DiMeG	1.3^c	179
$HgCl_2 \cdot$ 9-EtGH	1.0^c	147
$HgCl_2 \cdot$ guanosine^a	0.8	

[a] ^1H NMR study [21]. [b] Estimation only, due to problem with calculated Δ_{max} (see discussion in ref. 13a); estimated error ±0.3. [c] Estimated error ±0.1.

Supplemental material

Positional parameters and anisotropic temperature factors of **1** and **2**, a listing of observed and calculated structure factors and experimental details of the structure determinations can be obtained from the Fachinformationszentrum Karlsruhe, D-7514 Eggenstein-Leopoldshafen 2 under CSD 57251 on request. Requests should be accompanied by the complete literature citation.

Acknowledgements

We wish to acknowledge financial support by the Fonds der Chemischen Industrie and the Deutsche Forschungsgemeinschaft.

References

1 (a) J.-P. Charland, M. Simard and A.L. Beauchamp, *Inorg. Chim. Acta, 80* (1983) L57, and refs. therein; (b) S.E. Taylor, E. Buncel and A.R. Norris, *J. Inorg. Biochem., 15* (1981) 131, and refs. therein; (c) A.R. Norris, S.E. Taylor, E. Buncel, F. Bélanger-Gariépy and A.L. Beauchamp, *Inorg. Chim. Acta, 92* (1984) 271, and refs. therein; (d) W.S. Sheldrick and P. Bell, *Inorg. Chim. Acta, 160* (1989) 265, and refs. therein.

2 L.D. Kosturko, C. Folzer and R.F. Stewart, *Biochemistry, 13* (1974) 3949.

3 B.J. Graves and D.J. Hodgson, *Inorg. Chim., 20* (1981) 2223.

4 D.M.L. Goodgame, S.P.W. Hill and D.J. Williams, *Polyhedron, 11* (1992) 1507, and refs. therein.

5 J.A. Carrabine and M. Sundaralingam, *Biochemistry, 10* (1971) 292.

6 P. Lavertue, J. Hubert and A.L. Beauchamp, *Inorg. Chem., 15* (1976) 322.

7 M. Authier-Martin and A.L. Beauchamp, *Can. J. Chem., 55* (1977) 1213.

8 M. Authier-Martin, J. Hubert, R. Rivest and A.L. Beauchamp, *Acta Crystallogr., Sect. B, 34* (1978) 273.

9 N.Barba Behrens, B.A. Cartwright, D.M.L. Goodgame and A.C. Skapski, *Inorg. Chim. Acta, 31* (1978) L471.

10 M. Damodara Poojary and H. Manohar, *Inorg. Chim. Acta, 93* (1984) 153.

11 M.A. Romero-Molina, E. Colacio-Rodriguez, J. Ruiz-Sánchez, J.M. Salas-Peregin and F. Nieto, *Inorg. Chim. Acta, 123* (1986) 133.

12 S. Menzer, E.C. Hillgeris and B. Lippert, *Inorg. Chim. Acta, 210* (1993) 167.

13 (a) K.K. Finneiser, *Ph.D. Thesis,* Universität-Gesamthochschule Siegen, Germany, 1986; (b) L.G. Marzilli, B. de Castro, J.P. Caradonna, R.C. Stewart and C.P. van Vuuren, *J. Am. Chem. Soc., 102* (1980) 916.

14 G.M. Sheldrick, *SHELXTL PLUS* (Release 3.4), for Nicolet R3m/V crystallographic systems, University of Göttingen, Germany, 1987.

15 M. Nardelli, *Comput. Chem., 7* (1983) 95.

16 *International Tables for X-ray Crystallography,* Vol. IV, Kynoch, Birmingham, UK, 1974.

17 P.R. LeBreton, X. Yang, S. Urano, S. Fetzer, M. Yu, N.S. Leonard and S. Kumar, *J. Am. Chem. Soc., 112* (1990) 2138.

18 (a) H. Sternglanz and C.E. Bugg, *Science, 182* (1973) 833; (b) *J. Cryst. Mol. Struct., 8* (1978) 263.

19 B. Lippert, H. Schöllhorn and U. Thewalt, *Inorg. Chim. Acta, 198–200* (1992) 723.

20 (a) L. Brammer, J.M. Charnock, P.L. Goggin, R.J. Goodfellow, A.G. Orpen and T.F. Koetzle, *J. Chem. Soc., Dalton Trans.,* (1991) 1789; (b) I.C. M. Wehman-Ooyevaar, D.M. Grove, P. van der Sluis, A.L. Spek and G. van Koten, *J. Chem. Soc., Chem. Commun.,* (1990) 1367; (c) A.J. Blake, A.J. Holder, Y.V. Roberts and M. Schröder, *J. Chem. Soc., Chem. Commun.,* (1993) 260.

21 L.S. Kan and N.C. Li, *J. Am. Chem. Soc., 92* (1970) 4823.